Fluidized particle-in-tube solar receiver and reactor: A versatile concept for particulate calcination and high efficiency thermodynamic cycles

Cite as: AIP Conference Proceedings **2033**, 040017 (2018); https://doi.org/10.1063/1.5067053
Published Online: 08 November 2018

Jack Hoeniges, Inma Pérez-López, Hadrien Benoit, Daniel Gauthier, and Gilles Flamant

Fluidized Particle-In-Tube Solar Receiver and Reactor: A Versatile Concept for Particulate Calcination and High Efficiency Thermodynamic Cycles

Jack Hoeniges[1, 2], Inma Pérez-López[1, a)], Hadrien Benoit[1, b)], Daniel Gauthier[1], Gilles Flamant[1]

[1]*PROMES-CNRS, 7 Rue du Four Solaire, 66120 Font-Romeu, France*
[2]*Department of Mechanical Engineering, Valparaiso University, Valparaiso, IN 46383, USA*

[a)]Corresponding author: inma.perez@promes.cnrs.fr,
[b)] hadrien.benoit@promes.cnrs.fr

Abstract. This paper focuses on the concept of tubular Dense Particle Suspension solar receiver that consists in using solid particles transported by an air flow as heat transfer fluid. It was first developed for solar tower power plants but can also be applied for particulate thermal treatment. Experiments are being conducted on-sun at the CNRS 1 MW solar furnace in Odeillo. A first analysis of a stable experimental case is presented. A simplified model of the receiver is described and compared to the experimental case. The results show that the solar flux modeling is appropriate. The model needs to take into account the specific particle suspension flow pattern present in the absorber tube to be able to predict the temperatures of both particles and tube wall. A qualitative exploitation of the model predicts that the technology is appropriate for particulate decarbonation occurring at temperatures of 700 °C or below, but that it will be insufficient to achieve the complete decarbonation of particles reacting at 800 °C or above.

INTRODUCTION

Previous studies have proved the feasibility of an innovative tubular solar receiver that uses a Dense Particle Suspension (DPS) (class A particles, volume fraction around 30 %) as Heat Transfer Fluid (HTF). It is developed for solar tower power plants. This Upward Bubbling Fluidized Bed (UBFB) technology melds the fluidized bed advantages of efficient heat transfer and simple solid circulation with the good thermal properties of ceramic particles (high temperature sustained, high volume heat capacity). Two different solar rigs, a 10 kW_{th} single-tube receiver [1,2] and a 150kW_{th} multi-tube receiver [3] were successfully operated between 2013 and 2015 at the PROMES-CNRS 1MW solar furnace. A 750 °C outlet particle temperature was achieved during steady state with the single-tube set-up operated in batch [2]. The multi-tube rig, which allowed a continuous circulation, led to a 500 °C average temperature at the tubes' outlet with 700 °C for the hottest tube. The temperature was limited by the metallic tube material (stainless steel, maximum 900 °C).

In this study, a new experimental setup using a refractory alloy (Inconel 601) absorber tube (0.05 m OD, 1 m irradiated) is presented that allows a higher tube operating temperature (950 °C for long-term use, 1100 °C momentarily). Therefore, higher target outlet particle temperatures are achievable. In addition to high efficiency thermodynamic cycles, this opens the possibility of solar calcination (i.e. CaCO3, Cement Raw Mill, dolomite, phosphates). Temperature results are shown for one experimental case. A first interpretation is done. A simplified solar receiver-reactor model was developed to predict the setup behavior during on-sun tests and the achievable reactive powders chemical conversion. The model is described. Its validity is checked against an experimental case and a critical analysis is made. Finally, the model is exploited qualitatively.

SolarPACES 2017
AIP Conf. Proc. 2033, 040017-1–040017-8; https://doi.org/10.1063/1.5067053
Published by AIP Publishing. 978-0-7354-1757-1/$30.00

EXPERIMENTAL SETUP

Two dense Particle Suspension (DPS)-in-tube receivers have already been tested: a single-tube receiver [1,2] and a multi-tube receiver [3]. The current setup is an improved version of the single-tube receiver. It involves one single opaque tube containing the solid-gas dense suspension circulating upward. The general principle of this 1-tube solar receiver is illustrated in Fig. 1. The solar absorber is located inside a cylindrical cavity and subjected to concentrated solar radiation. The complete laboratory facility involves 2 fluid beds that enable the system to generate the suspension upward flow in the irradiated tube. The DPS moves upward vertically in the tube constituting the solar absorber thanks to the pressure difference imposed between the Dispenser Fluid Bed (DiFB) at the tube bottom and the Collector Fluid Bed (ColFB) at the tube top (ColFB at atmospheric pressure, DiFB around 200 mbar).

In order to operate the system in a closed loop, two modifications of the setup were tested. First, two rotary valves were installed at the inlet and outlet of the hopper (in this case, ColFB outlet connected to hopper inlet). The goal was to be able to pressurize the DiFB while feeding it from the hopper. However, the rotary valves allowed too large of an air flow passing through, which prevented the particles from the ColFB from coming back down. Second, a double-hopper system was installed with the hoppers alternatively filling and emptying. However, the piston-cylinders employed were not sufficiently air-tight. Due to the inability to achieve continuous circulation, the set-up was modified, and operated in batch circulation.

The absorber tube has an outside diameter of 0.05 m, a wall thickness of 0.002 m and is made of Inconel 601 coated with Pyromark® paint. It is subjected to the concentrated solar radiation over a 1 m height. Two tubes are currently being tested: a bare tube and a finned tube (8 longitudinal inside fins, 1.5 cm wide) to improve the heat transfer. The DiFB is equipped with six 1.5 kW electrical resistance heaters to uniformly preheat the fluidized bed before the particles flow into the solar absorber. The solid mass flow rate is controlled by a rotary valve. A gas analyzer and a solid sampling device will allow the determination of the chemical reaction yield, when working with reactive powders. The setup is equipped with more than fifty temperature and pressure sensors to follow the DPS and absorber tube wall heating, as well as the DPS density and solid inventory in the various setup elements. The thermocouples measuring the tube wall temperature are directly welded to it, which leads to very low thermal contact thermal resistance. In the case of two surfaces put in contact with a pressure exceeding of 10^7 Pa, the thermal contact resistance is in the range 0.7-4 m².K/W [4] and it is expected to be even lower for a contact by welding. Therefore, even if these thermocouples are directly exposed to the concentrated solar flux, the overestimation of the temperature was calculated to be lower than 2 %. These setup improvements compared to the earlier version are: a higher irradiated length (1 m instead of 0.5 m), a wider absorber tube (46 mm ID instead of 36 mm), an absorber material able to withstand higher temperatures, fins in the absorber tube, a higher maximum solid mass flux, more temperature measurements (front tube vertical temperature profile, DPS temperature at 5 radial positions at cavity inlet and outlet).

EXPERIMENTAL TESTS

The DPS-in-tube receiver reactor is currently being tested at the CNRS 1 MW solar furnace in Odeillo. A complete and detailed analysis of the results has not been done yet. Only some raw measurements for one experimental case with cristobalite (≈ 50 µm) and no fins is shown and interpreted here, with a mass flow of 381.6 kg/h, inlet temperature of 75°C and a average flux range of 213kW/m² to 376 kW/m². A stable solid circulation was established and the data was averaged over the stable time period (around 5 min). Table 1 shows the DPS temperatures at five positions at the cavity outlet and inlet respectively. At the outlet, the temperature does not change in the tube core (10 mm, 17 mm and 23 mm). The temperatures measured 3 mm from the wall at the tube front and back are higher than in the center with the front temperature being the highest. This temperature distribution is in agreement with the solid recirculation pattern previously evidenced [2]. The downward flow close to the wall is hotter than the upward flow in the center because the heat flux comes from the wall. At the inlet, the same distribution is observed with the core at uniform temperature and the wall at higher temperature. The temperature close to the tube front is 300 K hotter than in the core. This noticeable fact is due to the downward flow at the wall being heated all along the irradiated tube height from the cavity outlet to the inlet. In addition, the solar flux density impacting the tube is the highest at the tube bottom. Such significant temperature differences in the DPS at a given height are a new observation. While it may have existed in previous experiments it would go unnoticed because the thermocouples were further from the wall (5 mm before instead of 3 mm now). It is also logical that this difference is increased because the tube is wider and exposed to higher solar flux densities.

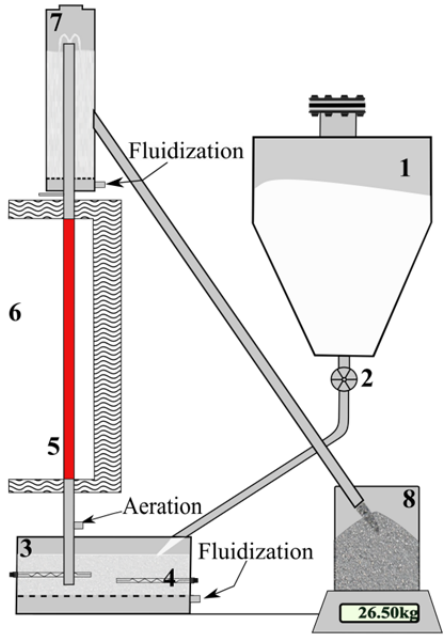

FIGURE 1. Experimental set-up cut view. 1. Hopper, 2. Rotary valve, 3. Dispenser Fluidized Bed (DIFB), 4. Electrical resistances, 5. Absorber tube, 6. Receiver cavity, 7. Collector Fluidized Bed (ColFB), 8. Container placed on weighing scale.

TABLE 1. DPS temperatures at the cavity outlet and inlet

		T_{inlet} [°C]	T_{outlet} [°C]
Distance from Back Wall	**3 mm**	88.9	266.7
	10 mm	61.0	216.6
	16 mm	62.0	212.2
	23 mm	72.8	210.3
Distance from Front Wall	**3 mm**	438.5	294.9

RECEIVER MODELING

Model Overview

Simplified models of the absorber tube and cavity were developed in order to supplement experimental results by predicting temperatures where measurements are not taken, such as particle temperature within the tube and tube temperature at various heights. The models were developed in MATLAB, and have varying degrees of complexity, in terms of discretization and the comprehensiveness of the heat transfer modeling. All models have a symmetry condition relative to the north-south vertical plan, and 20 discrete slices from top to bottom (over 1m for slice heights of 5 cm). The geometry is detailed in Fig. 2.

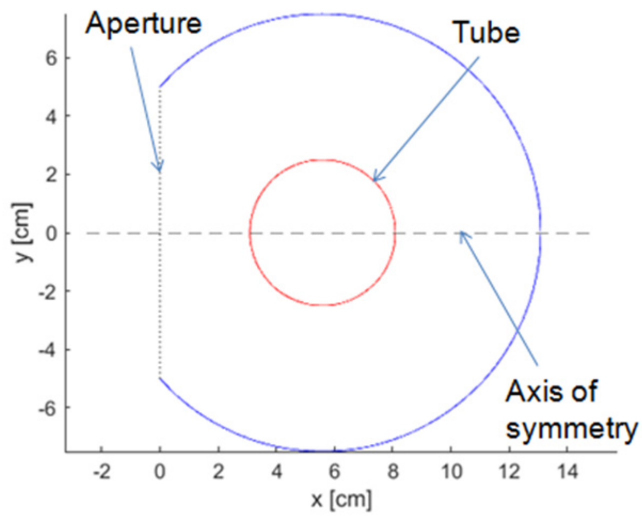

FIGURE 2. Top view of receiver geometry

Two different meshes were used. The coarser mesh divides the tube and cavity into two equally sized elements in each slice for a total of 80 elements between the tube and cavity, the finer mesh divides the tube and cavity into four equally sized elements for a total of 160 elements. Two different heat transfer models were tested. The simpler, 2D model neglects any heat transfer between the slices, making each slice its own thermally isolated system; the energy balance is thus easily described and resolved by a system of equations. A more complete 3D model of the system takes vertical heat exchanges into account using the Finite Volume Method. Both meshes were applied to the 2D and 3D models. None of the models take into account convective losses due to air circulating within the cavity. It was verified by ANSYS Fluent simulations that it only account for a few percents of the total heat distribution. The purpose of using different approaches and simplifications to develop different models was to provide validation for the assumptions taken to create the more basic models by comparing it to the more complete models.

Radiation Model

For all of the versions, radiation was modeled using the Monte Carlo ray tracing method (MCRT), a statistical approach well adapted to solar radiation problems, which can be configured for both two and three dimensional geometries. This method allows the user to represent radiation distribution more accurately than with a simple view factor, as it takes into account important surface and radiation properties, such as any directionality associated with the incoming solar radiation and spectral variations in surface absorptivity. In the presented models, the cavity absorptivity varied between solar and infrared radiation, and possible ray directions from the aperture were limited by the receptor geometry.

The MCRT method simulates the path of a bundle of thermal radiation energy from its surface of emission, to its surface of absorption, using probability distribution functions and a random number generator to calculate ray directions and determine when the ray is absorbed or reflected. By tracing a large number of rays emitted from each surface until their surface of absorption, the distribution factor (D) from surface i to surface j is calculated, as described by the equation below:

$$D_{ij} \equiv \frac{q_{ij}}{q_i} \cong \frac{N_{ij}}{N_i} \tag{1}$$

where q_{ij} is the amount of radiative energy emitted from surface i that is absorbed by surface j, and q_i is the total amount of radiative energy emitted from surface i. Using the MCRT, these quantities are approximated by N_{ij} (the number of simulated rays emitted from surface i that are absorbed by surface j) and N_i (the total number of rays emitted from surface i) respectively. These coefficients can then be used in conjunction with the Stefan-Boltzmann law and the known radiative flux at the aperture to calculate exactly how much infrared and solar radiation a receiver element absorbs from the rest of the receiver surfaces. An example of the results given by the MCRT is shown in Table 2.

TABLE 2. Distribution factors in percent from the 2D, coarser mesh model, calculated by simulating 10^4 rays from each surface

		Absorbed by				
		Tube Front	**Tube Back**	**Cavity Front**	**Cavity back**	**Aperture**
Emitted from	**Tube Front**	8.87	10.96	15.70	8.83	55.64
	Tube Back	9.40	23.48	16.82	23.25	27.05
	Cavity Front	19.03	20.38	10.39	12.25	37.95
	Cavity Back	8.39	34.22	11.61	15.61	30.17
	Aperture	74.87	9.99	1.88	4.20	9.06

Because this table applies to the 2D model, the distribution factors shown will not change with tube height. Conversely, with the three dimensional model, distribution factors vary with tube height, therefore each slice has its own, three dimensional distribution factor matrix to represent its radiative energy distribution throughout the receiver.

Comparison of Models

As mentioned previously, the simpler, two dimensional model neglects vertical heat transfer from slice to slice. This allows a very simple approach to temperature calculations, because each slice has its own system of equations, containing the same number of equations as elements, which can then be solved with relative ease. The model does not consider temperature gradients along the thickness of the tube or cavity walls, thus the temperature found on the exterior tube wall is considered to be the temperature seen by the dense particle suspension (DPS) flowing within the tube. Calculations begin at the bottom of the tube, where the DPS inlet temperature is known, the subsequently calculated tube temperature is used to find the change in DPS temperature between the inlet and outlet of the current slice. The convective heat transfer coefficient is calculated using a Nusselt number correlation established from the previous experimental results with a similar experimental setup [5]. The experiments conducted did not allow calculating a local value of the heat transfer coefficient but only a global one on the whole irradiated tube internal surface. It includes the radiation contribution, uses the bulk DPS temperature at the inlet and outlet (average of the temperatures measured in the tube center and 5 mm from the wall) and was necessarily determined for the specific DPS recirculation flow pattern. To account for the heat transfer increase caused by the fins, the convective heat transfer coefficient is multiplied by a coefficient. In a first approach, the coefficient used is 2. This will be adapted according to the experimental results. The process is then repeated for the following slice until all the temperatures along the height of the tube are known.

In order to validate the assumptions made for the simple model, a three dimensional model using the Finite Volume Method was developed. This model was coupled with a three dimensional Monte Carlo Ray Tracing model to consider all vertical radiation in addition to conduction exchanges. Though the tube and cavity temperatures are calculated differently compared to the previous model, they are calculated from top to bottom, allowing the same approach for DPS temperature calculation.

When comparing the different versions, one of the more interesting temperatures to consider is the maximum obtained tube temperature, which occurs on the front, south facing, tube exterior. Figure 3 below shows the model estimations of such temperatures for the first set of experimental parameters. It can be seen that the larger mesh models tend to yield lower maximum temperature, an affect that can be expected due to the averaging of the temperature over a larger surface area. Additionally it can be noted that for the majority of the height of the tube, the gap between models of different mesh size, is larger than the gap between models of different dimensions. This suggests that if the same mesh is applied, the more complex, three dimensional model may give only slightly different results for considerably more modeling effort. This effect becomes even more pronounced with parameters that lead to higher maximum tube temperatures. This trend lends confidence to the isolated slice assumption made for the two dimensional models, and suggests our efforts would be better directed towards creating models with finer meshes. Because of the finer resolution associated with the 4 element mesh, it will be used from here on to compare with experimental results.

The mesh study in itself is not complete. However it can already be seen that increasing the mesh resolution leads to an increase of the tube front temperature. This observation is linked to the averaging of the solar flux density over the cells surface area. The solar flux density is at its peak at the southernmost position and the further from this position, the lower the solar flux density. Therefore, the finer the mesh is, the higher the cell-averaged solar flux density gets, and so does the south wall temperature.

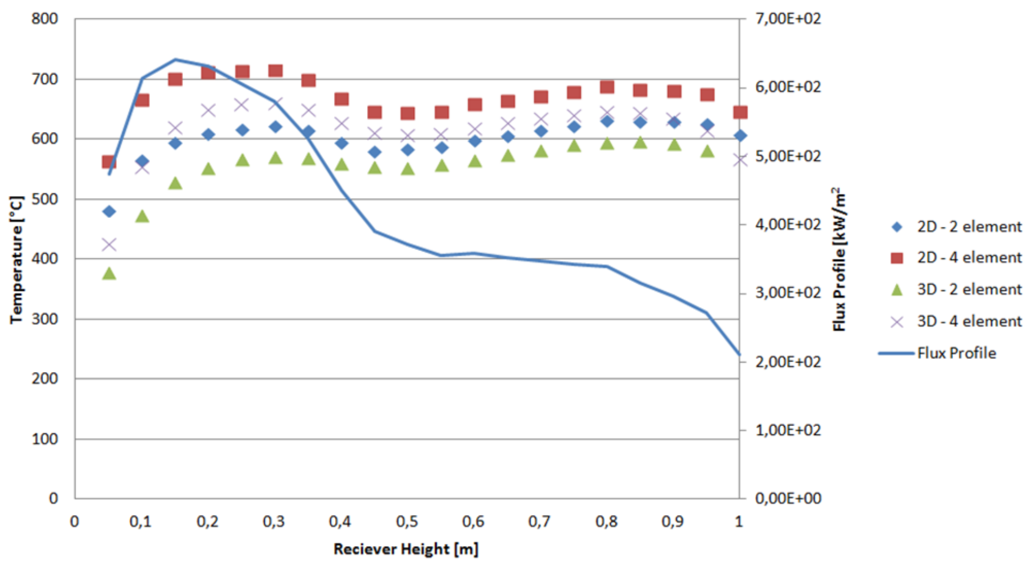

FIGURE 3. Applied solar flux and maximum tube temperatures (finned tube, cristobalite, 260 kg/h, and 243°C of preheating)

MODEL AND EXPERIMENTAL RESULTS COMPARISONS

The model results were compared to one experimental case. The inlet temperature, solid mass flow rate and solar flux density profile were set to reproduce the experimental conditions. As can be seen in Table 3, the model underestimates the power received by the DPS since the temperature increase between cavity inlet and outlet is 35 % lower in the model. This can be attributed to an underestimation of the heat transfer coefficient. Indeed, the Nusselt correlation used was determined in slightly different experimental conditions (tube height, diameter, particle material, solar flux densities) and is based on a global value of the heat transfer coefficient over the whole irradiated surface while it is applied locally in this study. Therefore, it is not surprising that the correlation is not perfectly adapted and requires adaptations. Figure 4 presents the front wall temperature profiles for a smooth tube, using the conditions presented in Table 3. The temperature measured at 0.25 m is not considered because its surprisingly low value was due to the thermocouple being broken. Figure 4 shows that the model greatly underestimates the wall temperature. Two reasons might explain this temperature underestimation. First, the mesh is probably not sufficiently refined and as we have seen, refining the mesh leads to a south wall temperature increase. Second, the experimental measurements showed that the DPS close to the front wall at the cavity inlet was 300 K higher than in the core. As was discussed in the experimental results section, the tube flow is subject to recirculation with the solid flow divided in an upward flow in the tube core and a downward flow close to the wall (annulus) (Note that the Nusselt correlation used was determined with this specific flow pattern). Consequently, the solid flowing downward close to the front wall gets much hotter than the rest of the solid in the tube. This explains the 300 K temperature difference at the cavity inlet. The wall exchanges heat with particles at the annulus temperature, while this temperature is not accessible by using the simplified plug-flow model that only calculates one solid temperature. Therefore, the model considers a heat exchange with a DPS whose temperature is, at the tube front, 300 K lower than it is actually. As a consequence, the difference between the modeled and measured temperatures at the front is almost the same as the temperature difference between the core and the DPS close to the front wall. The comparison of experimental and modeled temperatures of the tube wall at three heights, around the tube confirms that the model underestimates the wall temperature not only at the front but everywhere. This element definitely shows that the mesh refinement by itself would not solve the problem because while a finer mesh would increase the south temperature, it would decrease the temperatures over the rest of the circumference. Even though the modeled front wall temperatures are globally much lower than those measured, the profile shape is well reproduced. This validates the modeling method of the solar flux density.

TABLE 3. Experimental temperature results and corresponding model estimates

		T_{DiFB}	$T_{in,cav}$ [°C]	$T_{out,cav}$ [°C]	Mass Flow [kg/h]
	Experimental	16.7	75	217	
Smooth Tube	2D Model	-	75	179	381.6
	3D Model	-	75	172	

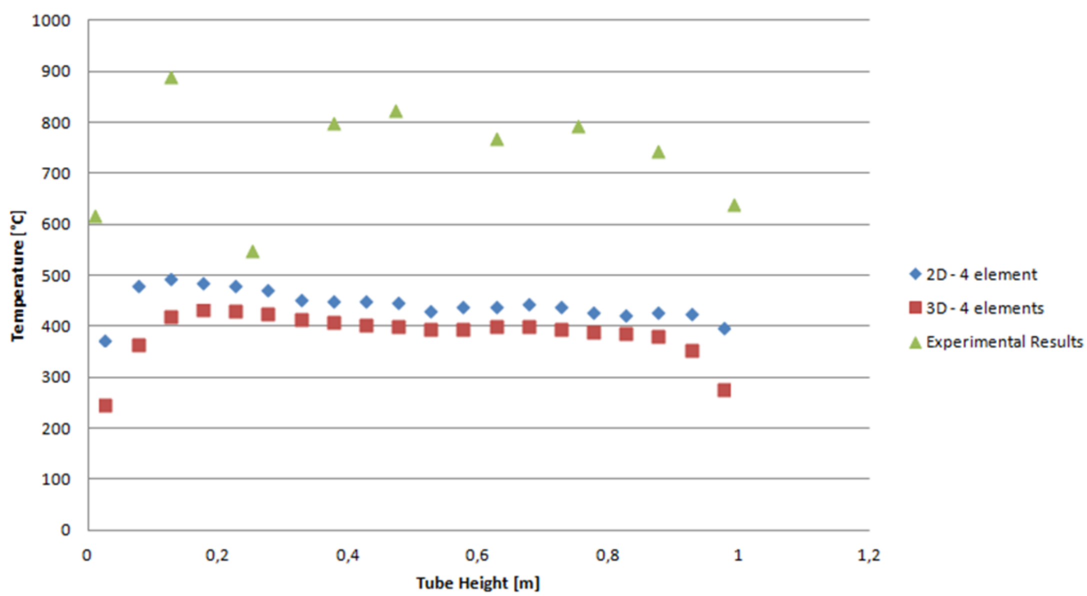

FIGURE 4. Maximum tube temperatures using a smooth tube with cristobalite flowing at 381.6 kg/h, and no preheating

MODEL EVALUATION AND EXPLOITATION

As it is, the model is not able to give accurate estimations of the temperatures. It underestimates the wall-to-DPS heat exchange and the wall temperature. The wall-to-DPS heat exchange can be corrected by improving the Nusselt correlation used. However, precise wall temperature estimation requires the knowledge of the DPS annulus temperature not calculated by the current model. This means that an accurate model has to take into account the DPS recirculation in the tube and the heat and mass exchanges between the core and the annulus.

The results currently given by the model being inaccurate, it is difficult to exploit it quantitatively. However, a qualitative exploitation was made in the case of calcium carbonate calcination. The predictions are that the particle-in-tube solar reactor is not appropriate for a complete calcination of $CaCO_3$. Indeed, with a maximum wall temperature of 950 °C (long-term use of Inconel 601), around 10 m of irradiated tube length is needed for a 95 % conversion. With the current setup that works in batch and has a 1 m irradiated tube length, a high conversion is impossible to achieve. This is due to the calcination of $CaCO_3$ that requires temperatures above 900 °C to have good chemical reaction kinetics. With a tube material able to sustain 1400 °C, the complete conversion could be achieved with a much smaller length (model prediction: 1.5 m). For other materials that have lower decarbonation temperatures, such as dolomite, the particle-in-tube solar reactor concept is expected to lead to high conversion ratios. This will be tried during the current experimental campaign.

CONCLUSION

A single-tube experimental DPS-in-tube receiver is being tested at the CNRS 1 MW solar furnace in Odeillo. It is a technology that allows reaching the temperatures necessary for high efficiency thermodynamic cycles or particle treatment. The setup is improved compared to former setups: higher irradiated length (1 m instead of 0.5 m), wider absorber tube (46 mm ID instead of 36 mm), absorber material able to withstand higher temperatures, fins in the absorber tube, a higher maximum solid mass flux, and more temperature measurements.

The first experimental results confirmed the recirculation pattern previously observed in the solid flow with an upward flow in the tube core and a downward flow close to the wall. A significant temperature difference, up to 300 °C, was observed between the DPS in the core and close to the front wall. This indicates that the heat transfer from wall to DPS is conditioned by the particle exchange between the annulus and the core.

Simplified models that consider a plug-flow were developed in MATLAB. The Monte Carlo ray-tracing method was used to determine the distribution factors in the receiver cavity. A 2D and 3D model, neglecting or not the vertical heat transfer were coded. Two meshes were tried. Using a refined or coarse mesh leads to differences much greater than between the 2D and 3D models. Therefore working with the 2D model and a refined mesh is a good option for a simple use combined with a good precision. For further improvement of the model, the mesh will have to be even more refined.

The plug-flow simplification renders the model unable to predict accurately the tube temperature because it does not consider the DPS temperature close to the wall, while it is with the particles at this temperature that the wall exchanges heat. Therefore, the model underestimates the wall temperature. A model that accounts for the recirculation flow pattern is necessary to obtain precise results.

A qualitative exploitation of the model tells us that the particle-in-tube reactor concept will not be appropriate for a complete decarbonation of calcium carbonate due to the high temperature needed for good reaction kinetics. To render the technology valid for $CaCO_3$, materials for the absorber tube able to sustain temperatures above 1000 °C in the long term are needed. However, the application to other powders that have lower decarbonation temperatures, such as dolomite or phosphates, seems promising and will soon be tested.

ACKNOWLEDGMENTS

This project has received funding from the European Union's Horizon 2020 research and innovation program under two grants agreements No 654663 and No 727762 projects acronym SOLPART and Next CSP, respectively. The facility was supported by the French "Investments for the future" program managed by the National Agency for Research under contracts ANR-10-EQPX-49 (SOCRATE).

REFERENCES

1. G. Flamant, D. Gauthier, H. Benoit, J. L. Sans, R. Garcia, B. Boissière, R. Ansart, M. Hemati, *Chem. Eng. Sci.*, 102 (2013) 567-576.
2. H. Benoit, I. Pérez-López, D. Gauthier, J.-L. Sans, G. Flamant, *Sol. Energy*, 118 (2015) 622-633.
3. I. Pérez-López, H. Benoit, D. Gauthier, J. L. Sans, E. Guillot, G. Mazza, G. Flamant, *Sol. Energy*, 137 (2016) 463-476.
4. T.L. Bergman, A.S. Lavine, F.P. Incropera, and D.P. DeWitt. Fundamentals of Heat and Mass Transfer. John Wiley & Sons, 7th edition, 2011. (Chapter 3, Table 3.1, p. 118).
5. H. Benoit. Tubular solar receiver with dense particle suspension upward flow (in French: Récepteur solaire tubulaire à suspension dense de particules en écoulement ascendant), Chapter 2, Doctorate Thesis, University of Perpignan Via Domitia (France), 2015.